

Protein Interactions Specific to Overexpressed G α 13: Effects of $\beta\gamma$ on Growth Signaling and Membrane Localization

Katherine M. Brown
Biology Department
The University of North Carolina Asheville
One University Heights
Asheville, North Carolina 28804

Faculty Advisor: Dr. Thomas E. Meigs

Abstract

The G12/13 class of heterotrimeric G proteins is unique in its ability to stimulate cellular transformation via overexpression of the wildtype α subunit, G α 12 or G α 13, absent of activating mutations. We have studied the mechanism of wildtype G α 12/13 signaling to the transcriptional activator Serum Response Factor (SRF), a pathway implicated in multiple cancer types. When overexpressed in cultured human embryonic kidney cells, wildtype G α 13 showed robust stimulation of this transcriptional response. This signaling by G α 13 was blunted by overexpression of G protein β 1 and γ 2 subunits, suggesting that aberrant signaling by the overexpressed α subunit results from stoichiometric imbalance between the heterotrimeric G protein subunits. Next, using an epitope-tagged G α 13 to track its subcellular location, we discovered the overexpressed α subunit shifted from a membrane-associated fraction to a soluble fraction, coincident with its sharp increase in SRF signaling. Overexpression of the β 1 γ 2 dimer caused re-localization of wildtype G α 13 to the membrane-associated fraction, coincident with its diminished signaling. Interestingly, our preliminary data utilizing a non-prenylated γ 2 subunit suggest the ability of the $\beta\gamma$ dimer to suppress signaling by overexpressed, wildtype G α 13 is independent of $\beta\gamma$ association with the cell membrane. We currently are examining effects of this non-membrane bound dimer on subcellular localization of wildtype G α 13. Furthermore, to characterize protein interactions specific to overexpressed G α 13, we have constructed Glutathione-S-Transferase (GST) fusions of several proteins reported as specific targets of G α 13, including RGS16, PYK2, and Talin-1. The role of G α 13 activation in binding these effector proteins will be examined by using aluminum, magnesium, and fluoride ions to chemically activate the α subunit.

1. Introduction

1.1 Background

The G-protein-coupled receptor (GPCR) protein family composes 4% of encoded human genes and is the largest family of cell surface receptors. The activation of GPCR-regulated signaling can lead to changes in gene transcription, apoptosis, cytoskeletal changes, and cell growth (O'Hayre et al. 2013). When the expression and activity of guanine nucleotide binding proteins (G proteins) and GPCRs becomes aberrant, tumorigenesis commonly occurs. Deep sequencing studies show that 20% of human tumors harbor mutations in GPCRs. The results of these studies indicate that G proteins and GPCRs have great potential in being novel therapeutic targets for cancer prevention and treatment (O'Hayre et al. 2013).

The activation of GPCRs involves the binding of a ligand at the extracellular side of the receptor; this binding induces a conformational change in the receptor and alters the position of its transmembrane helices and intracellular loops (O'Hayre et al. 2013). The conformational change resulting from the activation of the GPCR promotes the

release of GDP from the $G\alpha$ subunit, followed by the binding of GTP to the $G\alpha$ subunit and dissociation from $G\beta\gamma$ and from the receptor (Rosenbaum, Rasmussen, and Kobilka 2009).

The $G\alpha_{12/13}$ G protein subfamily is of particular interest, as it is the only subfamily that causes oncogenesis as an overexpressed, wildtype form. Mutations in the gene encoding G13, *GNA13*, are highly statistically significant in cancers that are derived from hematopoietic and lymphoid tissues, specifically in Burkitt's lymphoma and diffuse large-B-cell lymphoma (O'Hayre et al. 2013). Furthermore, meta-analysis of gene-expression microarray data sets revealed that $G\alpha_{13}$ is overexpressed in breast, oral, esophageal and colon cancers (O'Hayre et al. 2013).

1.2 Characterization of Protein Structure

In order to investigate how mutations in the $G\alpha_{12/13}$ G protein subfamily enhance cell proliferation and promote tumorigenesis, the structures of $G\alpha_{12}$ and $G\alpha_{13}$ must be elucidated. X-ray crystallography can explicate the complex three dimensional structure of proteins, however, accurately executing X-ray crystallography is extremely difficult, and requires the extensive investment of time, resources, and funding. However, there is an alternative to x-ray crystallography that is efficient and cost-effective. The characterization of the structure of a protein can be elucidated through the identification of its binding interactions. This can be done through the creation of Glutathione-S-Transferase (GST) fusion proteins that can subsequently be used in co-precipitation "pull-down" assays. The precipitant created through the assay is run through SDS-PAGE, transferred to a Western blot, and subsequently immunoblotted with either a $G\alpha_{12}$ or $G\alpha_{13}$ specific antibody to detect if binding occurred between the GST fusion protein and the designated α subunit. The first objective of this study was to generate new GST fusion proteins, that previous studies have shown to be specific to $G\alpha_{13}$, which could be used for future co-precipitation assays. The GST fusion proteins created include RGS16, PYK2, and Talin1.

1.3 Novel Downstream Targets of $G\alpha_{13}$ Signaling

RGS16 selectively inhibits the conformational changes evoked by activated $G\alpha_{13}$ (Johnson et al. 2003). A previous lab member, Uri Cho, created a GST fusion of RGS16 that was composed of amino acids 1-31, as it was deemed necessary and sufficient for inhibition of $G\alpha_{13}$ -mediated SRE.L activation (Johnson et al. 2003). This construct was difficult to encode as a detectable protein. As a result, the literature was revisited and it was determined that two RGS16 constructs would be created. The first construct consisted of amino acids 1-87, and the second construct contained the entire amino acid sequence of RGS16 was created.

Previous literature demonstrated that the GTPase-deficient form of $G\alpha_{13}$ triggers PYK2 kinase activity and PYK2 tyrosine phosphorylation (Shi et al. 2000). Additionally, it was shown that *in vivo* $G\alpha_{13}$, although not $G\alpha_{12}$, readily associates with PYK2. Thus, G-protein-coupled receptors via $G\alpha_{13}$ activation can use PYK2 to link to SRE-dependent gene expression (Shi et al. 2000). A GST fusion construct of PYK2 was created using the entire amino acid sequence of PYK2.

Talin1 is a large 235-kDa cytoskeletal protein composed of an N-terminal 45-kDa FERM (4.1, ezrin-, radixin-, and moesin-related protein) domain, also known as the talin head domain, and a series of helical bundles known as the rod domain (Schiemer et al. 2016). The talin FERM domain consists of four distinct lobes designated as F0–F3. Integrin binding and activation are mediated through the F3 region, a critically regulated domain in talin (Schiemer et al. 2016). Previous literature demonstrated that $G\alpha_{13}$ directly interacts with Talin, relieves its state of autoinhibition, and triggers integrin activation (Schiemer et al. 2016). Two GST constructs of Talin1 were created. Understanding the interactions that occur between $G\alpha_{13}$ and Talin1 are of importance, as cytoskeletal proteins have roles in supporting oncogenic growth factor receptor (GFR) signaling and GFR-dependent cancer cell migration and invasion (Hamidi and Ivaska, 2018). The first construct consisted of the amino acids that encode the FERM domains F2-3 as the literature demonstrated $G\alpha_{13}$ binds directly to the F3 lobe of Talin1. The second construct consisted of the amino acids that encode the FERM domain in its entirety (F0-F3).

2. Methods

2.1 GST Fusion Constructs

Oligonucleotides were designed to be compatible with the cDNA of RGS16. Oligonucleotides were created to specifically generate the desired two constructs of RGS16, RGS16 (entire) and RGS16 (1-87). The oligonucleotides were used in PCR to extract the desired cDNA from a human brain tissue cDNA library. The desired sequences were extracted, purified, and inserted into the PGEX.KG plasmid through the use of restriction enzymes and ligation.

A similar process was followed for generating the PYK2 GST fusion construct. The oligonucleotides were used in PCR to extract the desired cDNA from a human brain tissue cDNA library and a PYK2 cDNA library. The desired sequences were extracted, purified, and inserted into the PGEX.KG plasmid through the use of restriction enzymes and ligation. Restriction was completed on both PCR products and the PGEX-KG plasmid. Sequencing showed the PYK2 library to be *Rattus norvegicus*, thus the human PYK2 derived from the brain cDNA library was used.

The constructs for Talin1 were created through determining which amino acids compromised the lobes of Talin1's FERM domain. Separate oligonucleotides were designed for FERM domains 0-3 (F0-3) and FERM domains 2-3 (F2-3). A brain cDNA library was used in PCR, and the desired products were ligated into the PGEX.KG plasmid. Sequencing was conducted on each of the five GST fusion constructs to ensure accuracy.

2.4 Isolation of GST Fusion Constructs

BL21 (Gold) DE3 cells were used to generate the constructs. An aliquot of BL21 (Gold) DE3 cells were thawed on ice. After thawing, the cells were pipetted into the appropriate falcon tube. The desired DNA plasmid was diluted to a concentration of 10 ng/ μ L. 1 μ L of diluted DNA was added to the appropriate chilled Falcon tube and was dispensed directly into the cells. The cells were flicked gently to mix and placed deep in ice for 30 minutes. The cells were heat-shocked at 42°C for 20 seconds and then quickly placed back in the ice for 2 minutes. 0.6 mL of SOC medium was pipetted into each Falcon tube. Tubes were placed in a 37°C incubator and shaken at 230 rpm for about 1 hour.

80 μ L of each Falcon tube was pipetted onto a corresponding LB-Ampicillin plate. Autoclaved glass beads were used to spread the cells across the plate. The glass beads were disposed after use and the plates were kept in a 37°C incubator for 13 to 16 hours. To prepare for the GST-fusion isolation, 500-mL Luria broth (LB) cultures, in 1 L flasks, and 12-mL LB cultures, in 125 mL flasks, were autoclaved. Once the cultures had cooled, ampicillin was added to reach a final concentration of 75 μ g/mL in each sterile 12-mL LB flask. Each flask was inoculated using a single bacterial colony. The 12-mL flasks were shaken at 37°C, 220 rpm for 12-16 hours. Ampicillin was added to reach a final concentration of 75 μ g/mL in each sterile 500-mL LB culture. 6 mL of each small bacterial culture was pipetted into the appropriate 500-mL LB culture. The cultures were shaken at 37°C, and 220 rpm. Starting time was noted, and after 90 min, and then every 20 min thereafter, remove 0.7 mL from one of the large cultures was removed and the absorbance of the culture was checked at A600 nm using a spectrophotometer. LB absent of any bacterial growth was used to blank the spectrophotometer.

When the A600 reached 0.5 – 0.8, IPTG was added to a final concentration of 0.5 mM in each large culture. The cultures were then returned to the shaker at 37°C and 220 rpm and incubated for an additional 2.5 – 3.5 hours. Each 500-mL culture was divided into 3 large centrifuge bottles. The bottles were centrifuged at 4°C for 15 min, at 6000g, in a Sorvall F14 6x250 rotor. At the end of the centrifuge run, the supernatant from each bottle was poured into a Clorox beaker. Excess liquid was removed, and the tubes were placed on ice. 2.5 mL of GST Buffer A, containing P.I. mix at a 1:500 dilution, 2.3 M sucrose, 50 mM Tris pH 7.7, and 1 mM EDTA was added to each pellet. The tubes were kept in ice as the bacterial pellet was broken up using the same plastic 10-mL pipet that was used to add the GST Buffer A. When the pellet was mostly broken up, the pellet was triturated until the mixture was homogenous. This mixture was passed this to the second pellet with the same GST-fusion protein, stirred and triturated, then passed to the third tube with same pellet. The process was repeated for the third pellet. DTT was added to GST Buffer B, composed of 50 mM Tris pH 7.7, 10 mM KCl and 1 mM EDTA, to reach a final concentration of 1 mM, and P.I. mix was added at a 1:500 dilution. 10 mL of this solution was added to each bacterial sample. Tubes were swirled to mix.

4-5 mg of lysozyme powder was weighed out and added to the bottle. Bottles were swirled rapidly to mix, and the bottles were incubated on ice for about 1 hour and were briefly removed to swirl approximately every 10 min. 400 mL of T₅₀ED buffer (50 mM Tris pH 7.7, 1 mM EDTA, 1 mM DTT) was prepared and stored on ice. Each bacteria/lysozyme sample was transferred to a labeled Oak Ridge centrifuge tube on ice. 175 μ L of 10% sodium deoxycholate, 260 μ L of 1 M MgCl₂, and 25 μ L of 5 mg/mL DNase I were added to each Oak Ridge tube. The tubes were kept on ice and hand rocked every 2 minutes until the liquid reached a thinner viscosity. The tubes were then

spun at ~15,000 rpm, 4°C, in a Sorvall F13 14x50 rotor for 40 minutes. A stock bottle of glutathione-sepharose was rocked back-and-forth until completely suspended, and then 0.35 mL was placed into each of four labeled 15-mL sterile conical tubes. 14 mL of cold T₅₀ED Buffer was added to each tube. The tubes were flicked vigorously to suspend beads in liquid. Tubes were spun in the “Silencer” clinical centrifuge at 4°C for 3 min at 1300g. Supernatant was removed with a pipet without disturbing the pellets. This step was repeated twice more. After the final wash, pellets were left on ice with just a slight cover of liquid. The supernatant was decanted from each spun-down Oak Ridge tube into the correspondingly labeled 15-mL conical tube of washed glutathione-sepharose beads. These 15-mL conical tubes were placed on an Orbitron in a fridge for 45 min. The tubes were then spun for 3 minutes at 1300g, 4°C in the Silencer Centrifuge. Supernatant was pipetted off from each resulting pellet. 4 M NaCl was added to the T₅₀ED Buffer, to achieve a final conc. of ~150 mM NaCl. 14 mL of this buffer was added to each sepharose pellet. Tubes were flicked to mix and spun again for 3 min at 1300g, 4°C. and then remove supernatant was removed, and the wash was repeated thrice more. On the last wash, the liquid meniscus was left slightly higher than double the height level of the settled sepharose beads. The beads were divided (50 µL each) into 30-40 tubes. During this process, a 1 mL pipette was used to triturate frequently, to ensure uniformity of the 50-µl aliquots. The aliquots were frozen in liquid nitrogen and stored at -80°C.

2.5 Gamma Mutagenesis

Anchoring of the G protein $\beta\gamma$ dimer to the inner face of the plasma membrane requires a geranylgeranyl lipid, covalently attached to the γ subunit (Mumby et al., 1990). A two-stage PCR process was utilized to create a Cysteine-to-Serine substitution just upstream of the γ 2 C-terminus, disrupting its CAAX motif (amino sequence CAIL) and removing its attachment point for the lipid. Our PCR process created two initial fragments of the γ 2 cDNA with 19-bp overlap encompassing the Cysteine-to-Serine mutation, and subsequent PCR of these fragments yielded the full-length, mutated cDNA. This construct, designated here by its C-terminal SAIL sequence, was verified by sequencing.

2.6 Data Analysis

A Kruskal-Wallis, a non-parametric ANOVA, test was used with a post-hoc Nemenyi test with Chi-squared approximation to investigate if there was a statistical significance between the average SRE-L/renilla ratio of CAIL and SAIL.

3. Results

Because our lab group was limited in its capacity for testing $G\alpha$ 13 binding to downstream target proteins, the first goal was to engineer forms of these proteins that could be immobilized on Sepharose beads. We utilized PCR to amplify multiple regions of the RGS16 coding sequence, and ligated these into a plasmid expressing the protein Glutathione-S-Transferase (GST). After expression of these proteins in *E. coli*, we isolated cytoplasm and captured these GST-RGS16 constructs on Sepharose. As shown in Figure 1, these proteins were successfully immobilized and appear to migrate at their expected molecular mass. This process was repeated for the PYK2 GST-fusion constructs and the Talin1 constructs. Figures 2-3 illustrate that the generation and isolation of these constructs was successful.

The resulting co-precipitation assays with all five GST fusion proteins generated did not yield any visible indications of interaction with myc-tagged $G\alpha$ 13 wildtype or the QL variant myc-tagged $G\alpha$ 13. The QL variant of $G\alpha$ 13 is a constitutively activated form that consists of a mutation of a key glutamine within the Switch Region II to a leucine. It was decided that interactions could be potentially detected through an alternative method of transiently activating the $G\alpha$ 13 subunit through the use of generating cell lysates in the presence of aluminum, magnesium, and fluoride. Methods were derived from Singer, Miller, and Sternweis 1994.

$G\alpha$ 13 mediates signaling from specific G protein-coupled receptors (GPCRs) to downstream transcription factors that include SRF, which activates *c-fos* and other early-immediate genes via binding to the serum response element (SRE). Overexpressed wildtype $G\alpha$ 13 sharply increases growth signaling due to stoichiometric imbalance with β and γ subunits of the G protein heterotrimer, and that this signaling event is abrogated by a co-expressed β 1 γ 2 dimer. Previous data showed HEK293 cells transfected with increasing mass of plasmids encoding wildtype and constitutively active (QL) myc-tagged $G\alpha$ 13 caused a >20-fold increase in SRF-mediated transcription in cells exhibiting a <3-fold increase in levels of wildtype $G\alpha$ 13. It was hypothesized that overexpressed $G\alpha$ 13 could be

triggering growth signaling due to stoichiometric imbalance, such that $\beta\gamma$ subunit levels were insufficient to form heterotrimeric complexes with the overexpressed α subunits (Figure 4). Transiently co-expressed $\beta 1$ and $\gamma 2$ observed a loss of signaling by wildtype $G\alpha 13$ but not activated (QL) $G\alpha 13$. Constitutively GDP-bound $G\alpha 13$ (GA) provided a negative control for SRF signaling. Membrane and soluble fractions of HEK293 cells previously transfected with myc-tagged, wildtype $G\alpha 13$, and immunoblotted to detect both native (43 kDa) and recombinant (45 kDa) $G\alpha 13$ were generated; native $G\alpha 13$ was detected exclusively in the membrane fraction. However, a high percentage of overexpressed, wildtype $G\alpha 13$ was detected in the soluble fraction, and this protein was retrieved to the membrane fraction by overexpression of G protein $\beta 1$ and $\gamma 2$ subunits (Figure 5).

The second objective of this study was to investigate the mechanism of overexpressed wildtype $G\alpha 13$, examine if a soluble subset of overexpressed $G\alpha 13$ contributed to growth and tumorigenic signaling, and examine if $\beta\gamma$ overexpression impedes signaling of overexpressed $G\alpha 13$ by recruiting it from a soluble to a membrane-bound location in cells. Figure 6 illustrates a gamma subunit lacking a carboxyl-terminal CAAX motif (where C = cysteine, A = an aliphatic amino acid, and X = any amino acid) was generated to aid in the investigation of how a non-membrane-bound $\beta\gamma$ could affect overexpressed wildtype $G\alpha 13$ (Mumby et al. 2006). Both CAIL $\gamma 2$ and SAIL $\gamma 2$, when transiently co-expressed with $\beta 1$, observed a loss of signaling by wildtype $G\alpha 13$ (Figure 7). Figure 8 confirmed that the results were not due to an imbalance of expression across the transfected HEK293 cells. To determine statistical significance between the average SRE-L/renilla ratio of CAIL and SAIL, a Kruskal-Wallis test was used in tandem with a post-hoc Nemenyi test (Figure 9). The results of the test showed there was no significant difference between the means (df = 1, p-value = 0.99). Immunoblots of CAIL $\gamma 2 + \beta 1$ and SAIL $\gamma 2 + \beta 1$ were generated to determine where the dimer resided in the cell. The location of SAIL in the soluble fraction validates the inability of the construct to tether to the membrane (Figure 10).

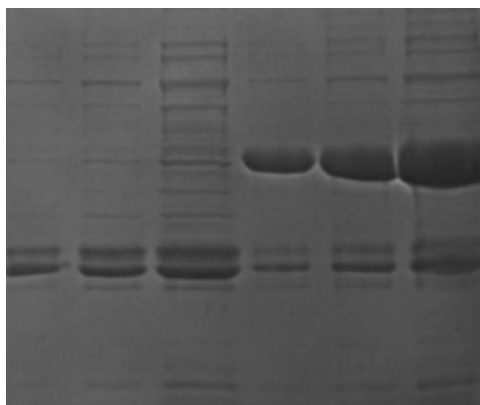


Figure 1. Coomassie Blue for confirmation of RGS16 (entire) and RGS16 (amino acids 1-87) constructs. A SDS-PAGE gel was run and subsequently stained with Coomassie Blue to confirm the presence of the GST constructs. Left to right illustrates varying concentrations of the constructs in order of 5 μ L, 10 μ L, and 20 μ L. First three left lanes are RGS16 (amino acids 1-87), and the rightmost lanes are RGS16 (entire).

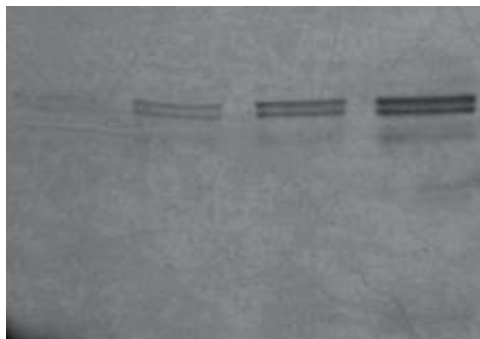


Figure 2. Coomassie Blue for confirmation of PYK2 construct. A SDS-PAGE gel was run and subsequently stained with Coomassie Blue to confirm the presence of the GST construct. Left to right illustrates varying concentrations of the constructs in order of 2 μ L, 5 μ L, 10 μ L, and 20 μ L.

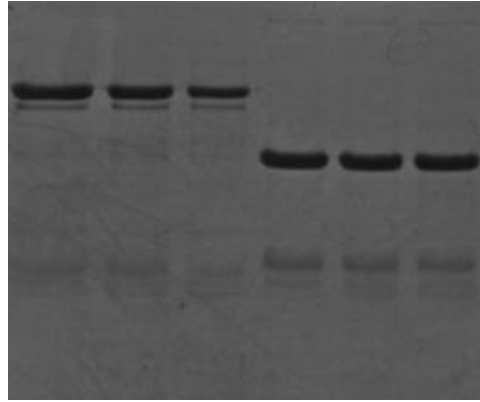


Figure 3. Coomassie Blue for confirmation of Talin1 (F0-3) and Talin1 (F2-3) constructs. A SDS-PAGE gel was run and subsequently stained with Coomassie Blue to confirm the presence of the GST constructs. The Leftmost three lanes show Talin1 (F0-3) construct with equal concentrations, and the rightmost three lanes show Talin1 (F2-3).

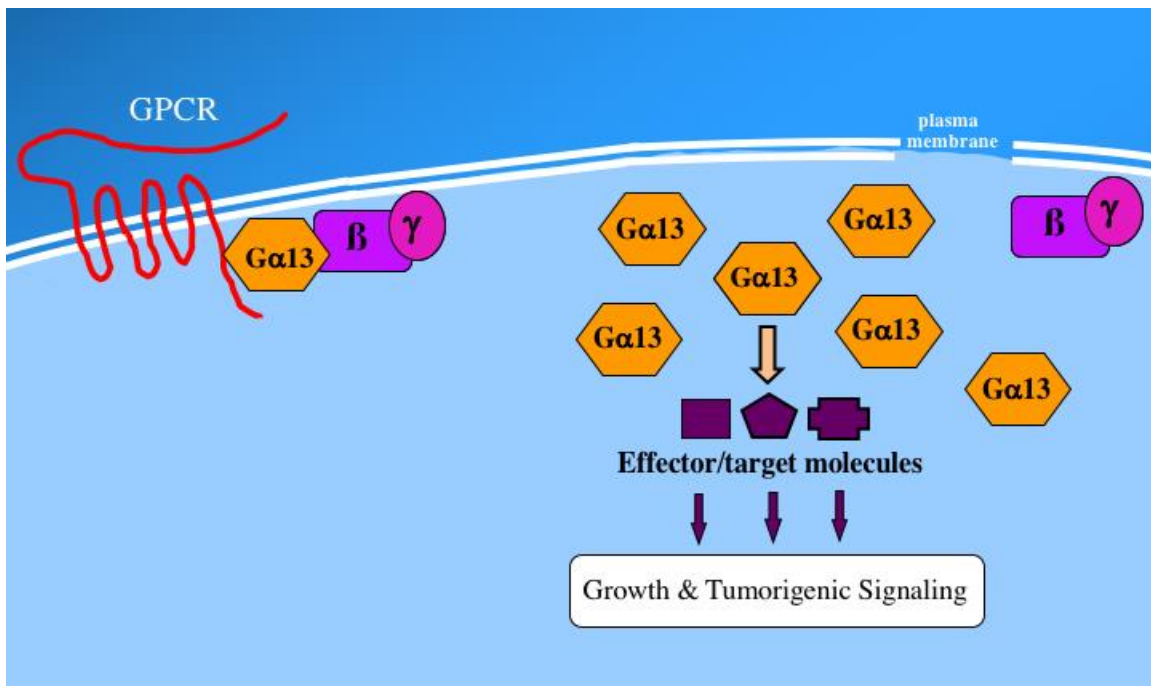


Figure 4. Theoretical model of overexpressed Gα13 driving cell growth and tumorigenesis due to stoichiometric imbalance. Gα13 mediates signaling from specific G protein-coupled receptors (GPCRs) to downstream transcription factors that include SRF, which activates c-fos and other early-immediate genes via binding to the serum response element (SRE). Gα13 and the closely related Gα12 have the unique property of driving proliferative signaling as overexpressed, wildtype forms without amino acid mutations.

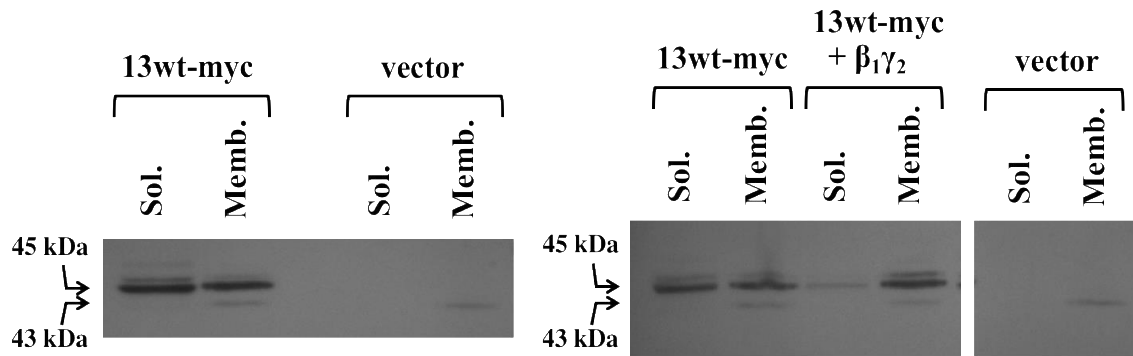


Figure 5. Overexpressed $G\alpha 13$ localizes to a soluble fraction, and is recruited to membranes by co-expressed $\beta 1\gamma 2$. We generated membrane and soluble fractions of HEK293 cells previously transfected with myc-tagged, wildtype $G\alpha 13$, and immunoblotted to detect both native (43 kDa) and recombinant (45 kDa) $G\alpha 13$. Native $G\alpha 13$ was detected exclusively in the membrane fraction. However, a high percentage of overexpressed, wildtype $G\alpha 13$ was detected in the soluble fraction, and this protein was retrieved to the membrane fraction by overexpression of G protein $\beta 1$ and $\gamma 2$ subunits.

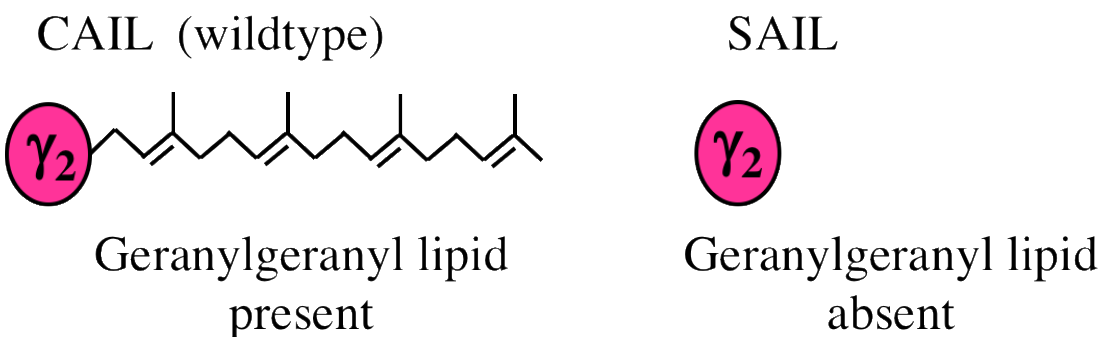


Figure 6. Construction of a $\gamma 2$ subunit lacking an isoprenylation site. Eliminating the CAAX motif through PCR directed mutagenesis was essential to eliminate the geranylgeranyl lipid necessary for association with the membrane. This “untethered” construct, designated here by its C-terminal SAIL sequence, was verified by sequencing.

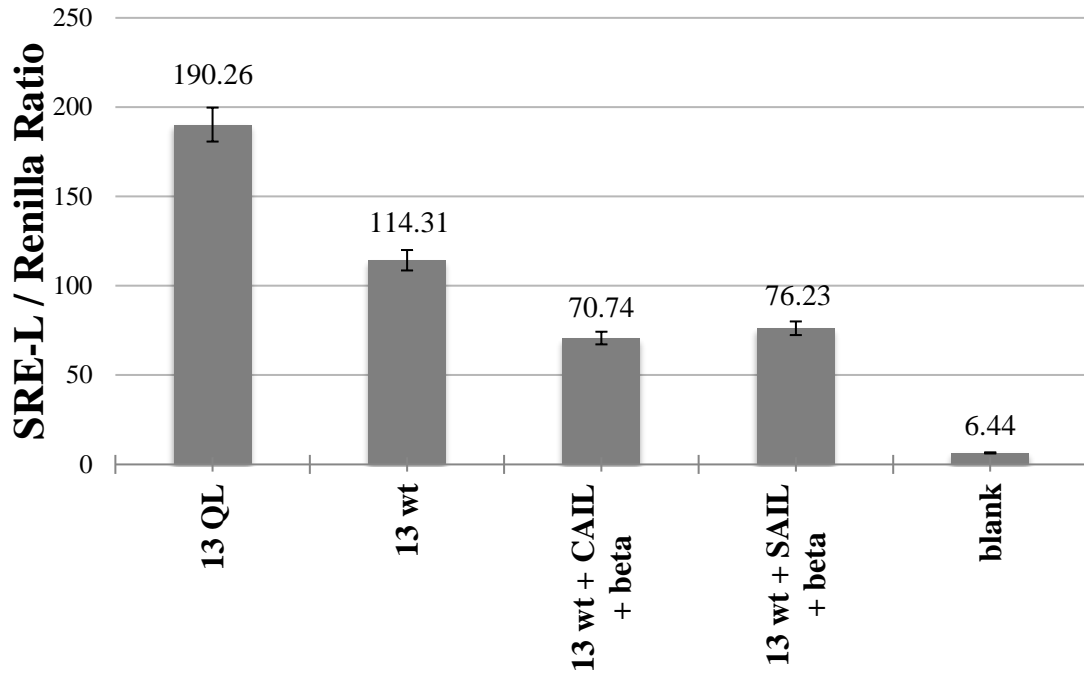


Figure 7. $\beta 1\gamma 2$ overexpression absent of its membrane anchoring is sufficient to suppress growth signaling by overexpressed $G\alpha 13$. The mean of seven independent experiments with duplicates of each sample is shown; error bars indicate range. The Promega Dual-Glo® luciferase assay system was utilized.

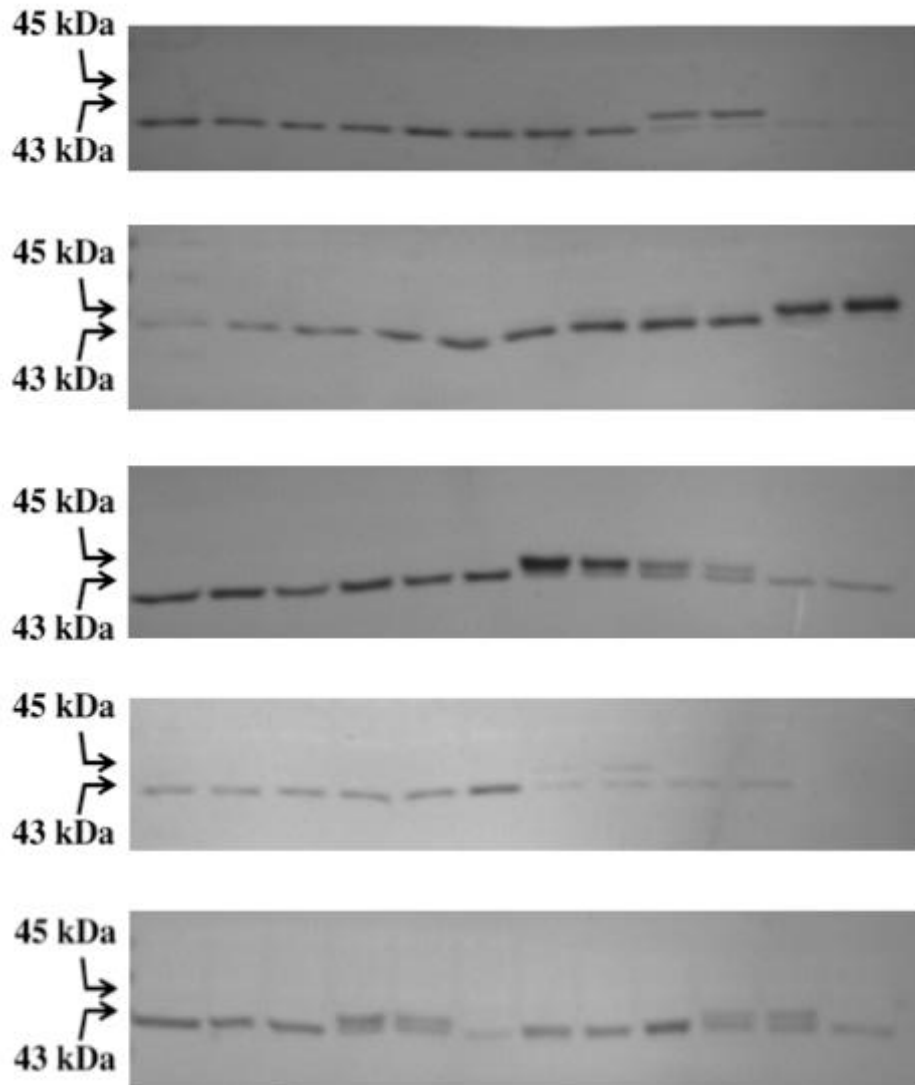


Figure 8. Passive Western blots of luciferase assays. Five representatives from the seven luciferase assays conducted were used to generate passive Western blots to examine even and equal expression across the transfected HEK293 cells. Examining equal expression is necessary to conclude that data was not due to any inability of the HEK293 cells to express the transfected DNA.

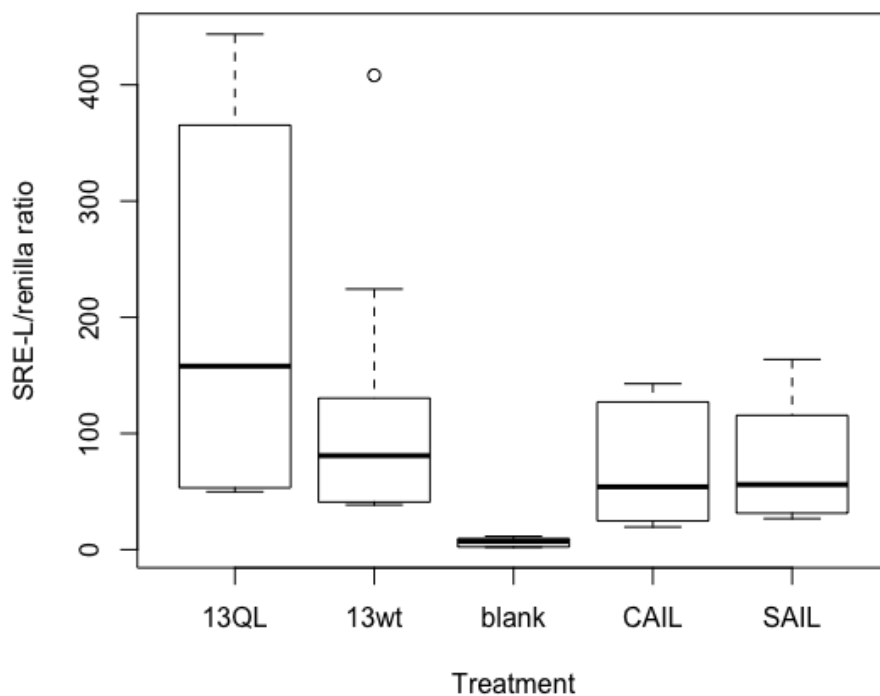


Figure 9. Box and whisker plot created using post-hoc Nemenyi test with Chi-squared approximation. A Kruskal-Wallis, non-parametric ANOVA test was used with a post-hoc Nemenyi test with Chi-squared approximation to investigate if there was a statistical significance between the average SRE-luciferase/Renilla luciferase ratio of the samples utilizing wildtype $\gamma 2$ (CAIL) vs. non-isoprenylated $\gamma 2$ (SAIL). Results of the test showed no significant difference between these means (df = 1, p-value = 0.99).

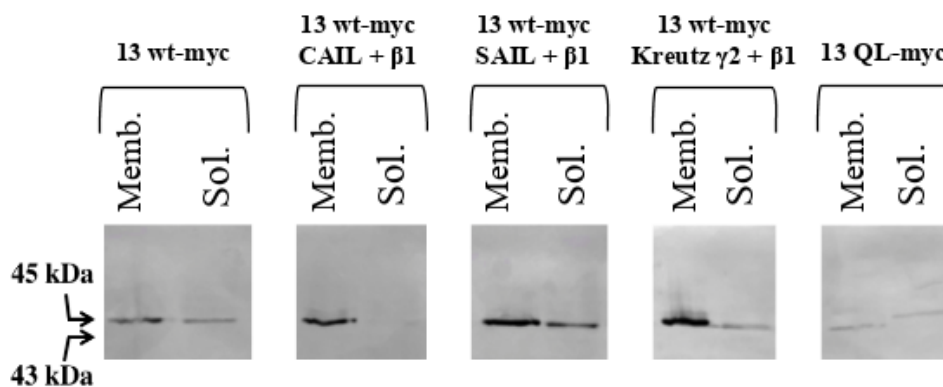


Figure 10. Effects of $\beta 1$ and non-isoprenylated $\gamma 2$ on subcellular localization of overexpressed $G\alpha 13$. Membrane and soluble fractions of HEK293 cells transfected with HEK293 cells previously transfected with myc-tagged $G\alpha 13$, myc-tagged $G\alpha 13$ QL, CAIL, SAIL, and Dr. Barry Kreutz's $\gamma 2$ were generated and immunoblotted. Similar

to Kreutz's $\gamma 2$, the majority of CAIL was found in the membrane, with a slight amount in the soluble fraction. SAIL was strongly detected in both the membrane and soluble fraction.

5. Discussion

A subset of overexpressed, wildtype $G\alpha 13$ drives aberrant growth signaling, via a mechanism possibly related to its mislocalization from membranes to a soluble fraction. Overexpressed $\beta 1\gamma 2$ partly suppresses $G\alpha 13$ signaling, concurrent with its recruitment of $G\alpha 13$ to membranes. The data generated through this study suggests that it is not necessary for the $\beta 1\gamma 2$ dimer to be membrane-tethered to dampen SRF signaling by overexpressed $G\alpha 13$.

Future direction of the investigation concerned with the characterization of the binding interactions of $G\alpha 13$ include the creation of additional $G\alpha 13$ specific GST fusion proteins such as AKAP110 (Carr, Dulin, and Voyno-Yasenetskaya, 2001). Co-precipitation "pulldown" assays with AMF lysates must be run. And all current GST fusion proteins should be tested alongside $G\alpha 12$ to ensure specificity to $G\alpha 13$. A potential approach to examining interactions between $G\alpha 13$ and PYK2 could include creating HeLa cell lysates due to the significant endogenous levels of PYK2 in HeLa cells (Shi 2000). The investigation of the gamma subunit should be furthered through the repetition of luciferase and fractionation assays. An investigation of if the $\beta 1\gamma 2$ dimer is specific to $G\alpha 13$ should be conducted to ensure that the heterodimer is not promiscuous. Additionally, an investigation of whether overexpressed $G\alpha$ subunits are bound to either GTP or GDP is of high interest.

6. Acknowledgements

I would like to acknowledge Dr. Meigs for giving me the opportunity to work in his lab, his guidance on this project, and his mentorship. I would like to thank Dr. Hale and Dr. Greene for being a part of my BIOL 498 committee, and I would further like to thank Dr. Hale for her assistance with my statistical analyses. I would also like to thank my fellow lab members for their support and encouragement. Thank you to the North Carolina Biotechnology Center, NC GlaxoSmithKline Foundation, and UNC Lineberger Comprehensive Cancer Center for funding and resources.

7. References

1. Carr, Daniel W, Nickolai Dulin, and Tatyana A Voyno-Yasenetskaya. 2001. "Interaction of Heterotrimeric G13 Protein with an A-Kinase- Anchoring Protein 110 (AKAP110) Mediates CAMP-Independent PKA Activation." *Current Biology* 11 (1): 1686–90.
2. Hamidi, H., and Ivaska, J. 2018. "Every step of the way: integrins in cancer progression and metastasis." *Nature Reviews Cancer* 18 (9): 533-548.
3. Johnson, Eric N., Tammy M. Seasholtz, Abdul A. Waheed, Barry Kreutz, Nobuchika Suzuki, Tohru Kozasa, Teresa L.Z. Jones, Joan Heller Brown, and Kirk M. Druey. 2003. "RGS16 Inhibits Signalling through the $G\alpha 13$ -Rho Axis." *Nature Cell Biology* 5 (12): 1095–1103.
4. Mumby, S. M., P. J. Casey, P. C. Sternweis, A. G. Gilman, and S. Gutowski. 2006. "G Protein Gamma Subunits Contain a 20-Carbon Isoprenoid." *Proceedings of the National Academy of Sciences* 87 (15): 5873–77.
5. O'Hayre, M., Vázquez-Prado, J., Kufareva, I. et al. 2013. "The Emerging Mutational Landscape of G Proteins and G-Protein-Coupled Receptors in Cancer." *Nature Reviews Cancer* 13 (6): 412–24.
6. Rosenbaum, Daniel M., Søren G. F. Rasmussen, and Brian K. Kobilka. 2009. "The Structure and Function of G-Protein-Coupled Receptors." *Nature* 459 (7245): 356–63.
7. Schiemer, James, Andrew Bohm, Glenn Merrill-Skoloff, Robert Flaumenhaft, Jin-Sheng Huang, Guy C. LeBrenton, and Athar Chishti. 2016. " $G\alpha 13$ Switch Region 2 Relieves Talin Autoinhibition to Activate AIIb $\beta 3$ Integrin."
8. Shi, C. S., S. Sinnarajah, H. Cho, T. Kozasa, and J. H. Kehrl. 2000. " $G13\alpha$ -Mediated PYK2 Activation. PYK2 Is a Mediator of $G13\alpha$ -Induced Serum Response Element-Dependent Transcription." *Journal of Biological Chemistry* 275 (32): 24470–76.

9. Singer, W. D., R. T. Miller, and P. C. Sternweis. 1994. "Purification and Characterization of the α Subunit of G13." *Journal of Biological Chemistry* 269 (31): 19796–802.